Materials Performance and Characterization

Enrico Lucon[1]

Review and Consideration of Apparent Negative Crack Growth in Fracture Toughness Tests

Enrico Lucon[1]

Review and Consideration of Apparent Negative Crack Growth in Fracture Toughness Tests

[1] National Institute of Standards and Technology, Applied Chemicals and Materials Division, 325 Broadway, Boulder St., CO 80305, USA (Corresponding author), e-mail: enrico.lucon@nist.gov, https://orcid.org/0000-0002-3021-4785

ABSTRACT

Apparent negative crack growth is often encountered when performing elastic-plastic fracture toughness tests with the Elastic Compliance single-specimen technique. It consists of a decrease of specimen compliance (reduction of crack size) during the early portion of the test, before the attainment of maximum force and the onset of ductile crack extension. This phenomenon was recognized and discussed inside the fracture mechanics community since the mid-1980s, but widespread consensus was never achieved on its root causes and on the best approach to account for it in the analysis of an elastic-plastic fracture toughness test. It has been shown that both experimental (test setup) and material behavior aspects can be invoked to explain the decrease of elastic compliance that translates into decreasing crack size in the early loading stage. The current edition of ASTM E1820, *Standard Test Method for Measurement of Fracture Toughness*, does not offer provisions to handle this phenomenon, and users are left free to treat the issue as they see fit. In this study, several articles published in the last 40 years were reviewed, and different proposed methods were applied on 15 selected tests performed on specimens of different geometries and thicknesses. Comparisons between original crack sizes, ductile crack extensions, and critical toughness values are presented, and recommendations are provided for revising ASTM E1820 with due consideration of the occurrence of apparent negative crack growth.

Nomenclature

α = ratio between crack size and specimen width, a/W

a = crack size, mm

a_o = measured initial crack size, mm

$a_{o,bl}$ = crack size before the onset of ductile crack initiation, accounting for crack tip blunting, used in Fernandez-Pisòn et al., mm

a_{oq} = predicted initial crack size, mm

B = specimen thickness, mm

b_o = initial uncracked ligament size, $W - a_o$, mm

C_m = measured elastic compliance, mm/kN

C_{th} = theoretical elastic compliance, mm/kN

Δ = difference between predicted and measured ductile crack extension, mm

Δ_{min} = minimum difference between predicted and measured ductile crack extension, mm

Δ_{max} = maximum difference between predicted and measured ductile crack extension, mm

$|\Delta|_{mean}$ = mean value of the absolute difference between predicted and measured ductile crack extension, mm

Δ_{mean} = mean value of the difference between predicted and measured ductile crack extension, mm

Δa = increase of crack size, or ductile crack extension, mm

Δa_o = difference between predicted and measured initial crack size, mm

$\Delta a_{o,min}$ = minimum difference between predicted and measured initial crack size, mm

$\Delta a_{o,max}$ = maximum difference between predicted and measured initial crack size, mm

$|\Delta a_o|_{mean}$ = mean value of the absolute difference between predicted and measured initial crack size, mm

$\Delta a_{o,mean}$ = mean value of the difference between predicted and measured initial crack size, mm

Δa_A = crack extension shift (adjustment) in the UTA method, mm

Δa_p = measured ductile crack extension, mm

Δa_{pred} = predicted ductile crack extension, mm

Δa_{shift} = correction for crack size/extension values in the CSS-1 method, mm

$f(\alpha)$ = function used in the CSS-1 method

F = correction function in the CSS-1 method (non-dimensional)

$F_{C(T)}$ = correction function in the CSS-1 method for C(T) specimens (non-dimensional)

$F_{SE(B)}$ = correction function in the CSS-1 method for SE(B) specimens (non-dimensional)

i = index of a specific data point in a J-R curve or fracture toughness data set

J = applied J-integral, kN/m

$J\text{-}R$ = crack resistance (curve)

J_{Ic} = critical fracture toughness according to ASTM E1820, kN/m

J_Q = provisional value of critical fracture toughness according to ASTM E1820, kN/m

N_{valid} = percentage of acceptable (valid) differences between predicted and measured initial crack sizes or ductile crack extensions

σ_f = flow strength, or average between yield and tensile strengths, MPa

T = test temperature, °C

W = specimen width, mm

Introduction

The phenomenon that is customary labelled "apparent negative crack growth" (ANCG) is often observed in the early stages of an elastic-plastic fracture toughness test conducted with the Elastic Compliance method. It consists in a nonphysical decrease of elastic compliance (corresponding to a decrease in crack size) before the onset of

ductile crack initiation. How to deal with this phenomenon in the analysis of the test, or the decision to ignore it completely, can significantly affect the results (critical fracture toughness J_Q/J_{Ic}, crack resistance curve).

ANCG has been acknowledged in the technical literature since the early 1980s with various interpretations and corrective measures, but a common understanding is still lacking, as well as a widely agreed-upon methodology for handling this phenomenon. The current version of ASTM E1820 at the time of writing (E1820-23b, *Standard Test Method for Measurement of Fracture Toughness*)[1] does not include specific provisions for dealing with this problem; the only reference to negative crack growth is in section 8.6.3.2, which reads: "If crack size values change negatively by more than 0.005 a_o (backup), stop the test and check the alignment of the loading train. Crack size values determined at forces lower than the maximum precracking force should be ignored." It is interesting to note here the use of "should" rather than "shall," which implies a recommendation rather than a requirement.

As a consequence, and in the absence of reliable guidance, many users resort to either (a) ignoring all data points before the minimum crack size, or (b) setting $\Delta a = 0$ for the shortest predicted crack size.

Various reasons and causes, both experimental and physical, for the occurrence of ANCG have been reported in the literature, including plastic indentation of compact tension, C(T), specimen holes, friction, misalignment of the loading train, specimen rotation, residual stresses developing during the unloading process, strain hardening of the plastic zone ahead of the crack tip, and crack tip blunting effects.

The aim of this study is to assess and compare various approaches for handling ANCG, and ultimately to recommend a specific approach to be implemented in a future ASTM E1820 revision.

Literature Review

The phenomenon of ANCG started to be acknowledged in the mid-1980s, when elastic-plastic fracture toughness testing was still in a relatively early development stage.

VOSS AND MAYVILLE (1983)

Voss and Mayville[2] presented elastic compliance results from 20 % side-grooved C(T) specimens of two different steels. The *J-R* curves that showed ANCG corresponded to specimens tested using clevises with round holes, whereas those tested with flat-bottomed holes did not exhibit negative crack growth. Based on previous research,[3] the authors claimed that the geometry of the clevis holes may determine the occurrence of ANCG for C(T) specimens, in case of round holes (when friction is largest) or whenever significant plastic indentation impedes the effective operation of flat-bottomed holes. As a practical solution, the use of hardened inserts between pins and clevis flats was recommended. An additional cause for ANCG was mentioned: time-dependent load relaxation effects, particularly at high test temperatures.

ROSENTHAL, TOBLER, AND PURTSCHER (1990)

Rosenthal, Tobler, and Purtscher[4] listed several causes for ANCG, such as friction, misalignment of the loading train, and physical blunting behavior effects. They proposed the following correction procedure for fracture toughness tests exhibiting ANCG.

(a) Fit all data points using:

$$\Delta a = K_1 J^{K_2} + K_3 \qquad (1)$$

where K_1, K_2, and K_3 are fitting coefficients, established by least squares regression.

(b) Shift all Δa values by K_3, i.e., $\Delta a' = \Delta a - K_3$.

Eqr{tkijv'd{"CUVO"ÏõyÕ°cñ'tkij w'tgugtxgf +'Ucv'Oct"2ó'ætæ2'sÑexfañ *Materials* Performance and Characterization
Fqy pnqcf gf Ir tkpvgf 'd{"
WU0'F GRV'QH'EQO O GTEG/P KUV'r wtuwncpv'q 'Negpug'Ci tggo gpv0'P q 'hwt yj gt 'tgr tqf wevkqpu'cwj qrk| gf 0

(c) Re-analyze the corrected $[\Delta a', J]$ values to determine the critical toughness and the crack resistance curve. Typically, the critical toughness J_{Ic} obtained after applying the correction procedure is higher than the original J_{Ic}.

UNDERWOOD, TROIANO, AND ABBOTT (1994)

The issue of ANCG for single-edge bend (SE(B)) specimens was addressed by Underwood, Troiano, and Abbott.[5] The correction procedure they suggested envisaged the following analytical steps.

(a) Select data points between 0.2 J_Q and 0.6 J_Q in the original data set, where J_Q is the provisional value of critical fracture toughness calculated from the original data set.

(b) Adjust all data points with $J \geq 0.2\ J_Q$ using the following crack extension shift:

$$\Delta a_A = \frac{\sum_i \left(\Delta a_i - \frac{J_i}{\sigma_f} \right)}{i} \tag{2}$$

where i is the number of data points with $J \geq 0.2\ J_Q$ and s_f is the material's flow stress (average of yield and tensile strengths at the test temperature).

(c) The adjusted data set is given by $(\Delta a_i', J_i)$, with $\Delta a_i' = \Delta a_i - \Delta a_A$.

Multiple iterations of the procedure outlined above are possible.

SEOK (2000)

In 2000, Seok[6] attributed ANCG to compressive residual stresses caused by the development of the plastic zone in front of the crack tip during the unloading process. He proposed the following two approaches for both C(T) and SE(B) tests.

Approach #1 (Compliance Correction)

Correct the measured unloading compliance, C_m, using

$$C_{\text{th}} = \frac{C_m}{1 - F} \tag{3}$$

where C_{th} is the theoretical unloading compliance, and F is a correction function given by

$$F_{C(T)} = \frac{\Delta P f^2(\alpha)}{\pi W B \sigma_Y} \left[\frac{(W - a)(2W + a)}{4(W^2 + aW + a^2)} - \frac{25(W + a)\Delta P^2 f^2(\alpha)}{128\pi W B^2 \sigma_Y^2 (W^2 + aW + a^2)} \right] \quad \text{for } C(T) \text{ specimens, and} \tag{4}$$

$$F_{SE(B)} = \frac{\Delta P S^2 f^2(\alpha)}{\pi W B \sigma_Y} \left[\frac{W - a}{2(W + a)} - \frac{25\Delta P^2 S^2 f^2(\alpha)}{96\pi W^3 B^2 \sigma_Y^2 (W + a)} \right] \quad \text{for } SE(B) \text{ specimens.} \tag{5}$$

In equations (4) and (5), $\alpha = \frac{a}{W}$, and the function $f(\alpha)$ is given by

$$f(\alpha) = \frac{(2 + \alpha)(0.886 + 4.64\alpha - 13.32\alpha^2 + 14.72\alpha^3 - 5.6\alpha^4)}{\sqrt{(1 - \alpha)^3}} \quad \text{for } C(T) \text{ specimens, and} \tag{6}$$

$$f(\alpha) = \frac{3\sqrt{\alpha}[1.99 - \alpha(1 - \alpha)(2.15 - 3.39\alpha + 2.7\alpha^2)]}{2(1 + 2\alpha)\sqrt{(1 - \alpha)^3}} \quad \text{for } SE(B) \text{ specimens.} \tag{7}$$

Approach #2 (Offset Technique)

The offset technique is based on the underlying principle that, during crack tip blunting,[*] J-Δa data points should lie on the blunting line.[†]

Based on this, all experimental crack growth values, Δa_i, should be offset by Δa_{shift}, with

$$\Delta a_{\text{shift}} = \frac{J_i}{\sigma_f} - \Delta a_{\text{min}}$$

(8)

J_{Ic} values obtained after correcting Δa_i values were found to be lower than before correction, and closer to the critical fracture toughness yielded by the multi-specimen approach.

WEISS AND NYILAS (2005)

Weiss and Nyilas[7] stated that ANCG is particularly significant for face centered cubic (FCC) materials, such as stainless steels, tested at cryogenic temperatures.

The cause of ANCG was attributed by the authors to strain hardening of the plastic zone ahead of the crack tip, which causes specimen stiffness to increase, and therefore compliance to decrease. Only after ductile crack initiation, stiffness starts decreasing. An additional cause mentioned is plastic deformation at the specimen sides, induced by the plane stress state that characterizes non-sidegrooved specimens.

The approach suggested by Weiss and Nyilas consists in placing the crack growth initiation point, which corresponds to the minimum compliance (maximum stiffness), onto the blunting line.

VERSTRAETE ET AL. (2014)

The occurrence of ANCG on single-edge tension, SE(T), specimens was addressed by Verstraete et al. in 2014.[8]

In the interpretation of the authors, the initial decrease of compliance preceding the onset of ductile crack extension should be attributed to the rotation of the two specimen halves for a stationary crack. Similar to Weiss and Nyilas,[7] the initiation of ductile crack extension is said to coincide with the compliance minimum.

The approach recommended by the authors is to first discard all data points before the compliance minimum and then shift the remaining data points by an amount corresponding to the crack tip blunting for the minimum compliance data point. For SE(T) specimens, blunting corresponds to half the crack-tip opening displacement (CTOD) up to stable crack growth initiation.

FERNÁNDEZ-PISON ET AL. (2021)

Fernández-Pison and coworkers[9] attempted various ANCG correction approaches on elastic-plastic fracture toughness tests performed at liquid nitrogen (77 K) and liquid helium (4 K) temperatures on disk-shaped compact, DC(T), specimens of AISI 304L and 316L stainless steels.

The approaches considered were as follows:

- The rigorous ASTM E1820 method, which contains no provisions for ANCG.
- The method proposed by Weiss and Nyilas.[7]
- A modified Weiss-Nyilas Compliance Method, consisting of an iterative application of the Weiss-Nyilas method. Starting from the measured initial crack size, a_o, the blunted initial crack size, $a_{o,bl}$, is updated until the difference between successive values drops below 10^{-5} mm.
- The Normalization Data Reduction Technique,[‡] which is standardized in Annex A15 of ASTM E1820.

---

[*]Crack tip blunting is a phenomenon whereby the material ahead of the fatigue crack tip plastically deforms upon the application of force. As a result, the crack tip blunts and the crack size somewhat increases, before actual ductile crack extension occurs.

[†]The increase of crack size during blunting as a function of applied J is represented by the so-called "construction line" (previously labeled "blunting line"), which according to ASTM E1820 follows the equation $J = 2\sigma_f \Delta a$.

[‡]The Normalization Data Reduction Technique[10] is used to obtain a J-R curve directly from a force-displacement test record, together with initial and final crack size measurements taken from the specimen fracture surface.

TABLE 1

Data sets considered in this investigation

Data Set ID	Geometry	a_o, mm	B, mm	W, mm	T, °C	Notes
ASTM-DS4	SE(B)	33.45	25.4	50.8	N/A	ASTM sample data sets[13]
ASTM-DS5	C(T)	29.97	25.4	50.8	N/A	
ASTM-DS7	SE(B)	27.91	25.4	50.8	N/A	
900HIP_4_N_a	PCCv	4.99	10	10	21	Precracked Charpy specimens[14]
AN-4-1	PCCv	5.23	10	10	21	
AS-4-3	PCCv	4.96	10	10	21	
CN-5-4	PCCv	5.12	10	10	21	
CN-8-3	PCCv	5.07	10	10	21	
BBL-CGW_23	C(T)	25.07	25.4	50.8	21	1TC(T) specimen[15]
W1-F11	PCCv	5.28	10	10	−196	Precracked Charpy specimens[16]
W2-F12	PCCv	5.16	10	10	−196	
W3-F6	PCCv	5.32	10	10	−269	
W4-F9	PCCv	5.20	10	10	−196	
FW1-A	SE(T)	2.62	11.8	11.8	21	B × B SE(T) specimens[17]
FH1-A	SE(T)	2.61	11.8	11.8	21	

The results reported indicated that the modified Weiss-Nyilas method was in good agreement with the Normalization Data Reduction Technique.

JAPANESE INDUSTRIAL STANDARD JIS Z 2284:1998

The only official test standard that explicitly addresses the issue of ANCG is the Japanese standard JIZ 2284,[11] which covers J_{Ic} testing of metallic materials in liquid helium.

The methodology prescribed in section 7.6.b.3 of the standard coincides with the procedure proposed by Weiss and Nyilas.[7] Data points are moved along the Δa axis in order to have the minimum value of Δa lie on the blunting line, expressed as $J = 2\sigma_Y \Delta a$.

Analyses Performed

In order to evaluate the effectiveness of the different published ANCG correction procedures listed above, 15 elastic-plastic fracture toughness data sets (**Table 1**) were selected. Three specimen geometries are represented (C(T), SE(B), precracked Charpy, PCCv, and SE(T)[*]), with nominal crack sizes ranging between 2.6 and 33.5 mm.

The seven correction approaches[†] detailed below were applied to the 15 data sets listed in **Table 1**.

(1) ASTM: analysis conducted in accordance with ASTM E1820 (no specific provisions for ANCG).
(2) Common Approach 1 (CA1): initial data points with $\Delta a > \Delta a_{min}$ (decreasing crack sizes) are deleted; crack growth values are not shifted or adjusted.
(3) Common Approach 2 (CA2): all crack growth values are shifted by an amount equal to Δa_{min}, so that the minimum crack growth is set equal to 0 and the minimum crack size is set equal to the measured a_o.
(4) Rosenthal, Tobler, and Purtscher[4] (RTP)
(5) Underwood, Troiano, and Abbott[5] (UTA)
(6) Chang-Sung Seok, Approach 1 – Compliance Correction[6] (CSS-1)
(7) Chang-Sung Seok, Approach 2 – Offset Technique[6] (CSS-2). This method is equivalent to Weiss and Nyilas[7] and JIS Z 2284:1998.[11]

[*]The single-edge tension, SE(T), geometry is presently not covered by ASTM E1820, although a specific ASTM test method is currently in preparation. The original analyses were performed according to the CANMET procedures,[12] and the same ASTM E1820 validity requirements used for C(T) and SE(B) specimens were applied to SE(T) specimens in this study.

[†]The two "Common Approaches" listed below (CA1 and CA2) do not have specific references associated but are the most frequently used techniques in fracture testing laboratories (in the absence of guidance from ASTM E1820) according to the experience of the author.

TABLE 2
Comparison between predicted and measured initial crack sizes. Acceptable and unacceptable predictions are highlighted in green and red, respectively

Data Set	Specimen Geometry	$a_{o,meas}$, mm	ASTM a_{oq}, mm	ASTM Δa_o, mm	CA1 a_{oq}, mm	CA1 Δa_o, mm	CA2 a_{oq}, mm	CA2 Δa_o, mm	UTA a_{oq}, mm	UTA Δa_o, mm	CSS-1 a_{oq}, mm	CSS-1 Δa_o, mm	CSS-2 a_{oq}, mm	CSS-2 Δa_o, mm
ASTM-DS4	SE(B)	33.45	31.26	−2.19	31.16	−2.29	33.54	0.09	31.33	−2.12	32.76	−0.69	31.38	−2.07
ASTM-DS5	C(T)	29.97	30.31	0.34	30.26	0.29	30.60	0.63	30.36	0.39	30.90	0.93	30.36	0.39
ASTM-DS7	SE(B)	27.91	27.56	−0.35	27.53	−0.38	27.56	−0.35	27.59	−0.32	28.80	0.89	27.59	−0.32
900HIP_4_N_a	PCCv	4.99	4.52	−0.47	4.52	−0.47	5.56	0.57	5.05	0.06	5.44	0.45	5.08	0.09
AN-4-1	PCCv	5.23	4.93	−0.30	4.63	−0.60	5.25	0.02	5.17	−0.07	5.09	−0.14	5.28	0.04
AS-4-3	PCCv	4.96	4.67	−0.29	4.35	−0.61	4.47	−0.49	4.87	−0.09	4.78	−0.18	4.88	−0.08
CN-5-4	PCCv	5.12	4.80	−0.33	4.45	−0.67	4.28	−0.84	5.17	0.05	4.92	−0.20	5.18	0.06
CN-8-3	PCCv	5.07	4.77	−0.29	4.47	−0.59	4.46	−0.61	5.03	−0.04	4.90	−0.16	5.12	0.06
BBL-CGW_23	C(T)	25.07	24.35	−0.72	24.30	−0.77	24.40	−0.67	24.52	−0.55	25.34	0.27	24.61	−0.46
W1-F11	PCCv	5.28	5.23	−0.05	5.23	−0.05	5.37	0.09	5.32	0.04	5.23	−0.05	5.23	−0.05
W2-F12	PCCv	5.16	5.01	−0.15	4.97	−0.19	5.01	−0.15	5.07	−0.09	5.13	−0.02	5.01	−0.15
W3-F6	PCCv	5.32	5.17	−0.15	5.12	−0.20	5.35	0.03	5.20	−0.12	5.25	−0.07	5.17	−0.15
W4-F9	PCCv	5.20	4.93	−0.27	4.88	−0.32	5.23	0.03	5.00	−0.20	5.05	−0.15	4.93	−0.27
FW1-A	SE(T)	2.62	2.51	−0.11	2.47	−0.15	2.65	0.03	2.45	−0.17	…	…	2.51	−0.11
FH1-A	SE(T)	2.61	2.46	−0.15	2.38	−0.23	2.66	0.05	2.64	0.03	…	…	2.46	−0.15

The metrics used to assess the effectiveness of each correction approach were based on the comparison between measured and predicted initial crack sizes (a_o and a_{oq}, respectively) and between measured and predicted ductile crack extension (Δa_p and Δa_{pred}, respectively) for each of the investigated data sets. Moreover, the scatter (spread) of the J_Q values calculated after applying each of the seven correction approaches was also evaluated.

Analysis Results and Discussion

INITIAL CRACK SIZE

Measured, a_o, and predicted, a_{oq},[*] initial crack sizes are compared in **Table 2**, which also reports calculated differences $\Delta a_o = a_{oq} - a_o$. Note that Seok[6] provided compliance correction factors only for C(T) and SE(B)[†] specimens, and therefore the CSS-1 method could not be applied to SE(T) specimens.

According to ASTM E1820-23a, section A9.4, if a_o and a_{oq} differ by more than the larger of $0.01W$ or 0.5 mm, the data set is considered not adequate according to the test method. In **Table 2**, acceptable and unacceptable predictions are highlighted in green and red, respectively. The general trends extracted from the analysis of **Table 2** are summarized in **Table 3**, which also includes average values of the absolute and relative differences between a_{oq} and a_o, $|\Delta a_o|_{mean}$ and $\Delta a_{o,mean}$, respectively.

The highest percentage of acceptable predictions (93 %) was returned by CSS-2, whereas CSS-1 yielded the lowest average difference between measured and predicted values, and UTA the lowest absolute difference. ASTM

---

[*]According to ASTM E1820-23b, a_{oq} is obtained by fitting all J_i and a_i data points before the specimen reaches the maximum force, using the following equation:

$$a = a_{oq} + \frac{J}{2\sigma_Y} + BJ^2 + CJ^3 \tag{9}$$

with a_{oq}, B, and C established by a least squares fit procedure.

[†]PCCv can be considered a single-edge bend specimen, and therefore the SE(B) compliance correction factor was used for tests on PCCv specimens.

Eqr {tki j v'd{ "CUVO "Ipy\ri*cm'tki j w'tgugtxgf +'Ucv'Oct'2\ "27<36<29'GFV'2'2ph *Materials Performance and Characterization*
Fqy pnqcf gf Ir tlpvgf "d{ "
WUL'OFGRV'QH'EQO O GTEG/P KUV'r wtuwcpv'vq 'Nkegpug'Ci tggo gpv0'P q 'hw't j gt'tgr tqf wevkqpu'cwj qtk| gf 0

TABLE 3

Effectiveness of six ANCG correction approaches for the prediction of initial crack size

Method	$|\Delta a_o|_{mean}$, mm	$\Delta a_{o,min}$, mm	$\Delta a_{o,max}$, mm	$\Delta a_{o,mean}$, mm	N_{valid}, %
ASTM	0.41	−2.19	0.34	−0.37	87
CA1	0.52	−2.29	0.29	−0.48	60
CA2	0.31	−0.84	0.63	−0.10	67
UTA	**0.29**	−2.12	0.39	−0.21	87
CSS-1	0.32	−2.62	0.93	**0.07**	77
CSS-2	0.30	−2.07	0.39	−0.21	**93**

Note: The best recorded metrics are shown in **bold green**. $|\Delta a_o|_{mean}$ = mean value of the absolute difference between a_{oq} and a_o; $\Delta a_{o,\ min}$, $\Delta a_{o,\ max}$ = minimum and maximum value of the difference between a_{oq} and a_o; N_{valid} = percentage of acceptable differences between a_{oq} and a_o according to ASTM E1820-23a.

FIG. 1

Comparison between measured and predicted initial crack sizes ($a_o < 5.5$ mm). The upper and lower dotted lines correspond to ±0.5 mm with respect to the equality between measured and predicted initial crack size.
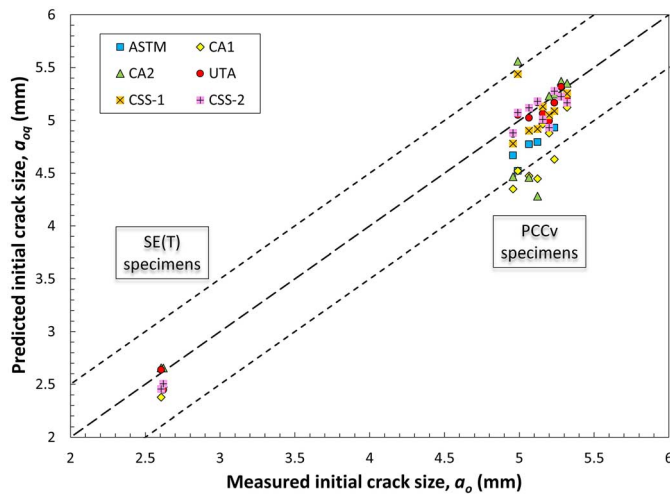
FIG. 2

Comparison between measured and predicted initial crack sizes ($a_o > 25$ mm). The upper and lower dotted lines correspond to ±0.5 mm with respect to the equality between measured and predicted initial crack size.

Eqr{tki j v'd{ "CUVO "Ko{nl"cm'tki j w'tgugtxgf +"Ucv'O ct"2*"42347533423'GV"hqt'tgr tqf wevkqpu'cwj qtk|gf0 *Materials Performance and Characterization*
Fqy pqcf gf Ir tkpvgf "d{"
WU0"F GRV'QH'EQO O GTEG/P KUV'r wtuwcpv'vq 'Nkegpug'Ci tggo gpv0P q'hwtyj gt'tgr tqf wevkqpu'cwj qtk|gf0
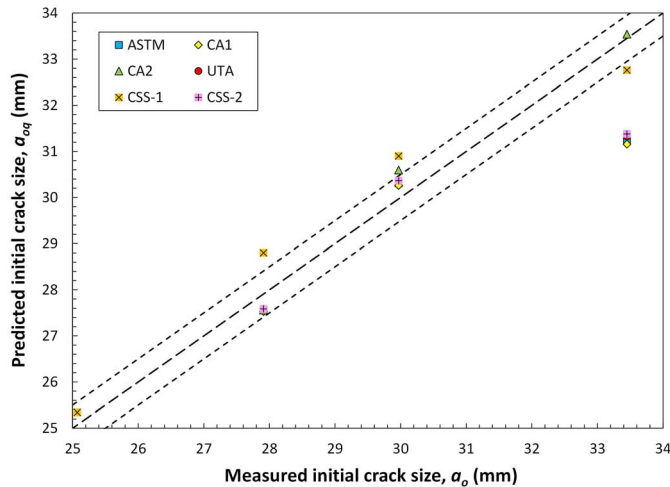
and UTA also exhibited a high percentage of acceptable predictions (87 %). The overwhelming tendency is for all correction approaches (with the exception of CSS-1) to underestimate the measured initial crack size.

Measured and predicted initial crack sizes are compared in **figure 1** (shorter cracks – SE(T) and PCCv specimens) and **figure 2** (longer cracks – C(T) and SE(B) specimens), with ±0.5 mm lines corresponding approximately to the acceptability band of ASTM E1820-23a.

DUCTILE CRACK EXTENSION

Measured, Δa_p, and predicted, Δa_{pred}, values of ductile crack extension at the end of test are compared in **Table 4**, along with differences $\Delta = \Delta a_{pred} - \Delta a_p$. Δa_{pred} is calculated as the difference between the predicted crack size corresponding to the last unloading and a_{oq}. Note that the RTP approach did not converge for two of the data sets analyzed.

Section 9.5.1.2 of ASTM E1820-23a prescribes that the difference between Δa_p and Δa_{pred} shall not exceed 0.15 Δa_p for crack extensions less than $0.2 b_o$, and $0.03 b_o$ thereafter, with $b_o = W - a_o$. For all 15 tests investigated, the latter criterion was used, as $\Delta a_p > 0.2\ b_o$ in all cases. Valid and invalid predictions are highlighted in **Table 4** in green and red/pink, respectively. An overall comparison of the seven correction approaches is shown in **Table 5**, which also includes average values of the absolute and relative differences between Δa_{pred} and Δa_p, $|\Delta|_{mean}$ and Δ_{mean}, respectively.

It can be immediately observed in **Table 5** that the general prediction quality is significantly worse for ductile crack extensions than for initial crack sizes (**Table 3**). The main reason for this is that the acceptability range is based on a small percentage (3 %) of the initial uncracked ligament size b_o, which is around 0.15 mm for PCCv specimens, which represent more than 50 % (9 out of 15) of the investigated data sets. Also, the method for estimating ductile crack extension also depends on the material's strain hardening, which is currently not accounted for in these predictions. Comparatively, the acceptability range for the initial crack size prediction is approximately ±0.5 mm for all the tests considered. It should also be noted that all average differences are negative, indicating that predictions tend to generally underestimate physical measurements, irrespective of the ANCG approach adopted. This was also generally observed for the predictions of initial crack size. Finally, we acknowledge that none of the considered approaches yielded acceptable ductile crack extension predictions for either SE(T) specimen, which is not covered by ASTM E1820.

TABLE 4

Comparison between predicted and measured ductile crack extensions. Valid and invalid predictions are highlighted in green and red/pink, respectively

Data Set	Specimen Geometry	Δa_p, mm	ASTM Δa_{pred}, mm	Δ, mm	CA1 Δa_{pred}, mm	Δ, mm	CA2 Δa_{pred}, mm	Δ, mm	RTP Δa_{pred}, mm	Δ, mm	UTA Δa_{pred}, mm	Δ, mm	CSS-1 Δa_{pred}, mm	Δ, mm	CSS-2 Δa_{pred}, mm	Δ, mm
ASTM-DS4	SE(B)	11.43	10.70	−0.73	10.80	−0.63	10.70	−0.73	11.03	−0.40	10.77	−0.66	10.25	−1.18	10.82	−0.61
ASTM-DS5	C(T)	12.60	12.42	−0.18	12.47	−0.13	12.13	−0.47	12.72	0.12	12.48	−0.12	13.03	0.43	12.48	−0.12
ASTM-DS7	SE(B)	7.45	7.05	−0.40	7.08	−0.37	7.05	−0.40	7.08	−0.37	7.08	−0.37	7.06	−0.39	7.08	−0.37
900HIP_4_N_a	PCCv	3.29	3.64	0.35	3.64	0.35	3.01	−0.28	3.24	−0.05	3.58	0.29	3.03	−0.26	3.61	0.32
AN-4-1	PCCv	2.33	2.61	0.28	2.91	0.58	2.30	−0.04	…		2.91	0.58	2.79	0.46	2.96	0.63
AS-4-3	PCCv	3.75	3.52	−0.23	3.84	0.09	3.72	−0.03	3.71	−0.04	3.73	−0.02	3.72	−0.03	3.73	−0.02
CN-5-4	PCCv	2.42	2.53	0.12	2.88	0.46	3.05	0.63	2.91	0.50	2.91	0.49	2.73	0.32	2.92	0.50
CN-8-3	PCCv	3.09	3.30	0.22	3.60	0.52	3.62	0.53	…		3.63	0.55	3.50	0.42	3.65	0.56
BBL-CGW_23	C(T)	3.87	3.58	−0.28	3.63	−0.23	3.58	−0.28	3.39	−0.47	3.74	−0.12	3.97	0.11	3.84	−0.02
W1-F11	PCCv	1.77	1.52	−0.25	1.35	−0.41	1.26	−0.51	1.35	−0.42	1.49	−0.27	1.50	−0.26	1.50	−0.27
W2-F12	PCCv	1.54	1.38	−0.17	1.42	−0.12	1.41	−0.14	1.38	−0.17	1.43	−0.11	1.43	−0.11	1.38	−0.17
W3-F6	PCCv	1.82	2.11	0.29	2.16	0.34	2.11	0.29	1.92	0.10	2.14	0.32	2.26	0.44	2.11	0.29
W4-F9	PCCv	0.96	0.45	−0.51	0.50	−0.45	0.45	−0.51	0.45	−0.51	0.52	−0.44	0.47	−0.49	0.51	−0.44
FW1-A	SE(T)	3.28	2.09	−1.19	2.11	−1.17	2.09	−1.19	2.51	−0.77	2.50	−0.78	…	…	2.60	−0.68
FH1-A	SE(T)	1.89	1.30	−0.60	1.38	−0.52	1.29	−0.60	1.30	−0.60	1.48	−0.41	…	…	1.38	−0.51

Eqr{tkijv'd{'CUVO"Kpvgtpcvkqpcnlu'tgugtxgf'"Ucv'Oct"2*Materials Performance and Characterization*
Fqy pnqcf gf lrtkpgf"d{"
WU0F GRV'QH'EQOOGTEG'P KUV"rwtuwcpv'q"Ncegpug'Ci tggo gpv0P q'hwtvj gt'tgrtqf wevkqpu'cwj qtk| gf0

TABLE 5

Effectiveness of seven ANCG correction approaches for the prediction of ductile crack extension

Method	$|\Delta|_{mean}$, mm	Δ_{min}, mm	Δ_{max}, mm	Δ_{mean}, mm	N_{valid}, %
ASTM	0.39	−1.19	0.35	−0.22	27
CA1	0.43	−1.17	0.58	−0.11	33
CA2	0.44	−1.19	0.63	−0.25	40
RTP	**0.30**	−0.77	0.50	−0.24	**54**
UTA	0.37	−0.78	0.58	−0.07	33
CSS-1	0.38	−1.18	0.46	**−0.04**	38
CSS-2	0.37	−0.68	0.63	−0.06	27

Note: The best recorded metrics are shown in **bold green** over light green background.

FIG. 3

Comparison between measured and predicted ductile crack extensions ($\Delta a_p < 4$ mm). The upper and lower dotted lines correspond to ±0.5 mm with respect to the equality between measured and predicted ductile crack extension.
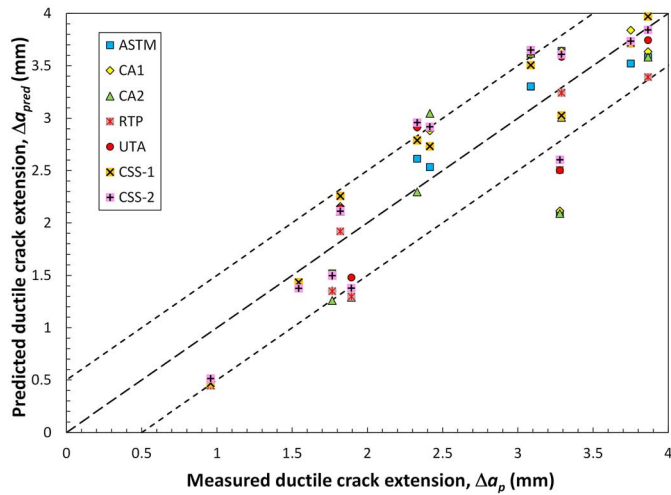
FIG. 4

Comparison between measured and predicted ductile crack extensions ($\Delta a_p > 7$ mm).

Eqr{tkijv'd{'CUVO'Kpvitc"*tcnkjw'tgugtxgf+"Ucv'Oct"2*Materials*"Performance*Performance and Characterization
Fqy pnqcf gf Irtkpvgf "d{"
WLF'FGRV'QH'EQOOGTEG/PKUV'*r wtuwcpv'q'Nlegpug'Citggo gpv0P q'hwtijgt'tgrtqfwevkqpu'cwj qtk| gf 0
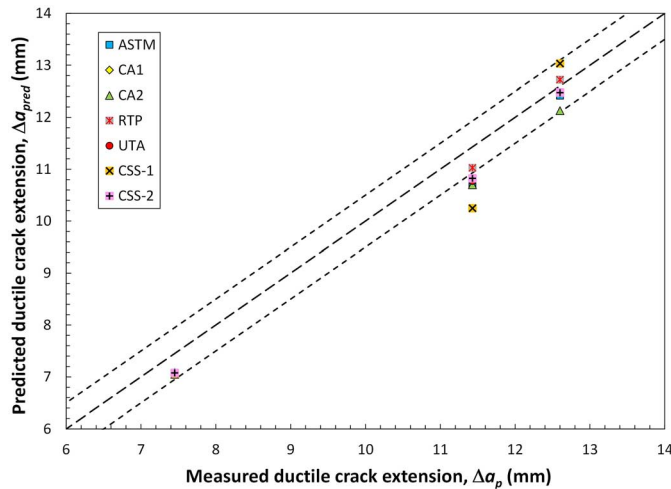
Based on **Table 5**, the most effective approach appears to be RTP, which exhibited the smallest absolute deviation and the highest percentage of valid predictions. However, the fit quality of the experimental data using equation (1) was often questionable, and in two cases (**Table 4**) was deemed unacceptable for further analyses.

Measured and predicted ductile crack extensions are compared in **figure 3** ($\Delta a_p < 4$ mm) and **figure 4** (7 mm $< \Delta a_p < 13$ mm). Short-dashed lines corresponding to a ± 0.5-mm prediction band are shown in both figures, which corresponds to the approximate ASTM **E1820** acceptability range, as mentioned above.

CRITICAL FRACTURE TOUGHNESS

For every investigated data set and ANCG correction approach considered, the provisional value of critical fracture toughness, J_Q, was calculated. The J_Q values obtained are collected in **Table 6**, which also reports the following parameters: J_Q spread for each data set, given by $(J_{Q,max} - J_{Q,min})/J_{Q,mean}$, and average J_Q values across the 15 data sets for each of the correction approaches.

In the last four rows of **Table 6**, the average values of J_Q for each correction approach over the examined data sets are provided, considering all the possible combinations of approaches for which calculations are available (listed in the leftmost cells). The point of these last four rows is to assess the possible tendency of each individual approach to over- or under-estimate J_Q, considering homogeneous subsets (i.e., groupings of the same approaches). For example, the last row of **Table 6** displays mean J_Q values over the first 13 data sets, for which CA2 and RTP results are not available.

Examination of **Table 6** leads to formulate the following observations.

(a) Large differences in the calculated values of critical fracture toughness are caused by the use of different ANCG correction approaches, as indicated by spread values as high as 103 % (data set ASTM-**DS4**) and an average spread of 40 % across the 15 investigated data sets.

TABLE 6
Values of provisional fracture toughness, J_Q, calculated in this investigation

Data Set	Specimen Geometry	J_Q, kN/m							Spread
		ASTM	CA1	CA2	RTP	UTA	CSS-1	CSS-2	
ASTM-DS4	SE(B)	38.85	31.81	38.85	5.58	37.09	37.92	35.57	103 %
ASTM-DS5	C(T)	32.43	31.13	…	21.97	30.83	35.93	30.83	46 %
ASTM-DS7	SE(B)	205.98	198.13	206.15	228.94	199.77	170.95	199.95	29 %
900HIP_4_N_a	PCCv	135.03	135.03	195.86	168.14	101.85	189.05	134.95	62 %
AN-4-1	PCCv	101.99	97.91	106.44	…	49.04	105.22	39.08	81 %
AS-4-3	PCCv	112.93	78.73	95.30	…	95.09	113.68	45.40	76 %
CN-5-4	PCCv	196.84	170.51	144.90	…	159.72	194.66	154.38	31 %
CN-8-3	PCCv	163.82	140.77	133.79	…	146.05	161.93	128.88	24 %
BBL-CGW_23	C(T)	779.49	768.65	770.12	806.25	723.91	674.91	655.99	20 %
W1-F11	PCCv	228.13	281.43	302.75	282.57	237.59	267.04	235.75	28 %
W2-F12	PCCv	236.15	224.73	228.71	239.66	221.48	240.24	223.85	8 %
W3-F6	PCCv	96.08	86.76	96.08	113.61	89.02	97.85	86.87	28 %
W4-F9	PCCv	204.71	198.73	204.71	205.20	197.47	208.76	197.57	6 %
FW1-A	SE(T)	1,063.30	945.81	1,392.99	1,199.33	1,204.60	…	923.86	42 %
FH1-A	SE(T)	1,847.71	1,730.46	1,657.98	1,873.07	1,553.72	…	1,739.44	18 %
ASTM,CA1,UTA,CSS-2		362.90	341.37	…	…	336.48	…	322.16	40 %
ASTM,CA1,RTP,UTA,CSS-2		442.53	421.15	…	467.67	417.94	…	405.88	…
ASTM,CA1,CA2,UTA,CSS-2		386.50	363.53	398.19	…	358.32	…	342.97	…
ASTM,CA1,UTA,CSS-1,CSS-2		194.80	188.02	…	…	176.07	192.16	166.85	…

Note: In the bottom part of the table, the highest and lowest average values for a specific combination of correction approaches are highlighted in red/pink and brown/yellow, respectively. Boldface indicates the average value of spread across the data sets investigated.

Eqt ('tii j vü ('CUVO ''kv#%nlki j u#'jngrxgf +'Ltv'Ot c' 2Materials Performance and Characterization''
Fqy pnjcf gf''I'tbpgf ''ti''"
Wl DF GRVQHI'EQ QO GTEG P HUV't wncpv'vq'Nlegpug''C1 ggo gpv'OP q'hwvj gt't grt tqf'wctkpcm''cw1k gf 0

TABLE 7

Overall performance of six ANCG correction approaches in terms of fractional errors (f.e.) and J_Q deviations

Data Set	$a_{o,meas}$, mm	Δa_p, mm	CA1 a_o f.e.	Δa_p f.e.	ΔJ_Q, %	CA2 a_o f.e.	Δa_p f.e.	ΔJ_Q, %	RTP Δa_p f.e.	ΔJ_Q, %	UTA a_o f.e.	Δa_p f.e.	ΔJ_Q, %	CSS-1 a_o f.e.	Δa_p f.e.	ΔJ_Q, %	CSS-2 a_o f.e.	Δa_p f.e.	ΔJ_Q, %
ASTM-DS4	33.45	11.43	−0.045W	−0.012W	18	0.002W	−0.014W	0	−0.008W	86	−0.042W	−0.013W	5	−0.014W	−0.023W	2	−0.041W	−0.012W	8
ASTM-DS5	29.97	12.60	0.006W	−0.003W	4	0.012W	−0.009W	…	0.002W	32	0.008W	−0.002W	5	0.018W	0.008W	−11	0.008W	−0.002W	5
ASTM-DS7	27.91	7.45	−0.008W	−0.007W	4	−0.007W	−0.008W	0	−0.007W	−11	−0.006W	−0.007W	3	0.018W	−0.008W	17	−0.006W	−0.007W	3
900HIP_4_N_a	4.99	3.29	−0.047W	0.035W	0	0.057W	−0.028W	−45	−0.005W	−25	0.006W	0.029W	25	0.045W	−0.026W	−40	0.009W	0.032W	0
AN-4-1	5.23	2.33	−0.06W	0.058W	4	0.002W	−0.004W	−4	−0.233W	…	−0.007W	0.058W	52	−0.014W	0.046W	−3	0.004W	0.063W	62
AS-4-3	4.96	3.75	−0.061W	0.009W	30	−0.049W	−0.003W	16	−0.004W	…	−0.009W	−0.002W	16	−0.018W	−0.003W	−1	−0.008W	−0.002W	60
CN-5-4	5.12	2.42	−0.067W	0.046W	13	−0.084W	0.063W	26	0.05W	…	0.005W	0.049W	19	−0.02W	0.032W	1	0.006W	0.05W	22
CN-8-3	5.07	3.09	−0.059W	0.052W	14	−0.061W	0.053W	18	−0.309W	…	−0.004W	0.055W	11	−0.016W	0.042W	1	0.006W	0.056W	21
BBL-CGW_23	25.07	3.87	−0.015W	−0.005W	1	−0.013W	−0.006W	1	−0.009W	−3	−0.011W	−0.002W	7	0.005W	0.002W	13	−0.009W	−0.0004W	16
W1-F11	5.28	1.77	−0.005W	−0.041W	−23	0.009W	−0.051W	−33	−0.042W	−24	0.004W	−0.027W	−4	−0.005W	−0.026W	−17	−0.005W	−0.027W	−3
W2-F12	5.16	1.54	−0.019W	−0.012W	5	−0.015W	−0.014W	3	−0.017W	−1	−0.009W	−0.011W	6	−0.002W	−0.011W	−2	−0.015W	−0.017W	5
W3-F6	5.32	1.82	−0.02W	0.034W	10	0.003W	0.029W	0	0.01W	−18	−0.012W	0.032W	7	−0.007W	0.044W	−2	−0.015W	0.029W	10
W4-F9	5.20	0.96	−0.032W	−0.045W	3	0.003W	−0.051W	0	−0.051W	0	−0.02W	−0.044W	4	−0.015W	−0.049W	−2	−0.027W	−0.044W	3
FW1-A	2.62	3.28	−0.012W	−0.099W	11	0.003W	−0.101W	−31	−0.065W	−13	−0.015W	−0.066W	−13	−0.222W	−0.278W	…	−0.01W	−0.057W	13
FH1-A	2.61	1.89	−0.019W	−0.044W	6	0.004W	−0.051W	10	−0.05W	−1	0.003W	−0.035W	16	−0.221W	−0.16W	…	−0.013W	−0.044W	6
Average values			−0.031W	−0.002W	7	−0.009W	−0.013W	−3	−0.049W	2	−0.007W	0.001W	10	−0.031W	−0.027W	−3	−0.008W	0.001W	15

(b) The average values of J_Q shown in the last rows of **Table 6** illustrate which of the seven investigated approaches tends to provide the lowest (most conservative) and largest (least conservative) values of critical toughness. The mean values to be compared must obviously be obtained from the same correction approaches, considering that for some data sets and correction approaches a J_Q value could not be determined (empty cells). **Table 6** indicates that the CSS-2 approach consistently provides the most conservative critical toughness values. The conservatism, with respect to the average value for a specific combination of correction approaches, ranges between 5.4 and 9.1 %.

Considering that errors in critical toughness are directly affected by individual errors in the predicted values of a_o and Δa_p, **Table 7** allows assessing the overall performance of six ANCG approaches with respect to the current ASTM E1820 procedure, by displaying the fractional errors (expressed in terms of specimen width, W) in the estimates of initial crack size and ductile crack extension, as well as the percentage J_Q deviations with respect to the values calculated according to ASTM E1820. The average values in the last row of **Table 7** show that UTA and CSS-2 provide the lowest fractional errors for both a_o and Δa_p. RTP is the approach that corresponds to the lowest mean deviation with respect to ASTM E1820.

Recommendations for a Future Revision of ASTM E1820

When the phenomenon of ANCG was first acknowledged in the scientific literature, the causes were mainly attributed to experimental effects, such as friction between pins and C(T) specimen holes, plastic indentation of the holes or loading clevises, misalignment of the loading train, etc.[2–4] Successive investigations pointed the finger at additional material-related effects, such as compressive residual stresses in the plastic zone during the crack tip blunting phase and strain hardening of the material ahead of the crack tip that causes specimen stiffness to increase (and therefore compliance to decrease).[4,6,7] Rotation effects occurring for a stationary (non-growing) crack and necking were also mentioned in the case of SE(T) specimens.[8]

Several authors[6–9] concur in claiming that the point of minimum compliance, i.e., minimum estimated crack size on the J-R curve, corresponds to the initiation of ductile crack propagation. This data point should therefore be placed on the so-called blunting line, which represents the apparent increase of crack size in the early stages of a fracture toughness test because of the plastic deformation of the crack tip and the formation of a plastic zone ahead of the fatigue precrack. This correction approach, which was identified as CSS-2 in this study, corresponds to the method prescribed by the only official test standard which explicitly addresses ANCG.[11] Based on the

FIG. 5

Comparison between provisional critical toughness values calculated in accordance with ASTM E1820-23b and using the CSS-2 correction approach.

Eqr{tkijv'd{''CUVO"Fpvgtpcvkqpcnkljvu'tgugtxgf+''Ucv'Oct'20'22*38<22"GFV'4244*
Fqypnqcfgf'Irkpvgf'd{"
WUO'FGRV'QH'EQOOGTEG'PKUV'rwtuwcpv'vq'Nkegpug'Citggogpv0Pq'hwtvjgt'tgrtqfwevkqpu'cwvjqtk|gf0*

Materials Performance and Characterization
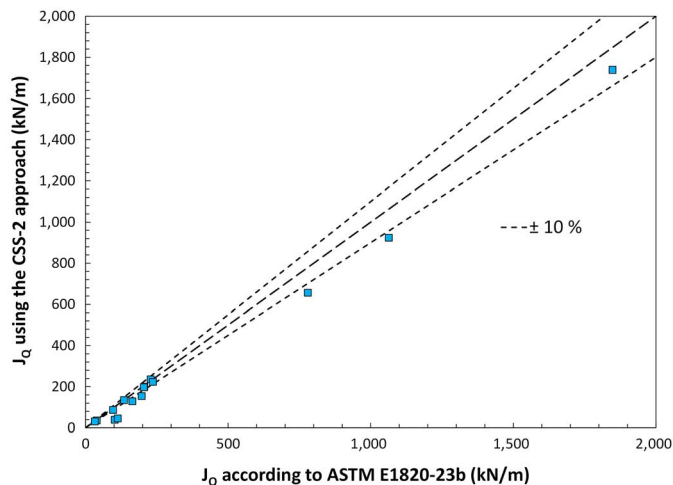
analyses presented here, this approach provides a high number of acceptable predictions of initial crack size, is equivalent to other methods in terms of ductile crack extension prediction, and yields generally conservative estimates of critical fracture toughness. The conservatism of CSS-2 with respect to the current ASTM E1820 procedure tends to increase with the toughness level (see **fig. 5** for a direct comparison between J_Q values from ASTM E1820-23b and CSS-2). We recommend the implementation of the CSS-2 correction method in a future revision of ASTM E1820.

Regardless of the specific approach preferred, the current provisions of ASTM E1820-23b (stopping the test and checking the alignment of the loading train, as well as ignoring crack size values determined at forces lower than the maximum precracking force) do not sufficiently address the issue of ANCG in the author's opinion, even though loading train alignment is certainly an important experimental aspect that must be adequately addressed.

Conclusions

Based on the review of the scientific literature on the topic of apparent negative crack growth occurring in the early stages of elastic-plastic fracture toughness tests conducted with the elastic compliance technique, it appears clear that this phenomenon is caused by a combination of experimental factors (friction, misalignments, etc.) and material-related effects (residual stresses, strain hardening, crack tip blunting effects, etc.). The proof of this lies in the fact that this phenomenon is not observed on all materials and all test temperatures, but only for certain materials and test temperatures (for example, austenitic stainless steels tested at cryogenic temperatures).

Our investigation, which considered seven different ANCG correction approaches, selected from the literature, applied to 15 *J-R* data sets from various specimen geometries and dimensions, showed that the resulting spread of critical toughness values, J_Q, is significant and can be as high at 103 %. The current provisions of ASTM E1820, which substantially ignore ANCG, appear technically unjustified and can sometimes lead to unconservative results.

Notwithstanding that aspects related to the test setup must always be adequately addressed, the ANCG correction approach that we recommend for inclusion in a future revision of the ASTM Test Method (labeled as CSS-2 in this study) consists in discarding all data points before the minimum predicted crack size and placing the data point corresponding to the minimum compliance on the blunting line, as it corresponds to the initiation of ductile crack propagation. This approach has been proposed by several authors, is prescribed by a Japanese test standard on J_{Ic} testing of metallic materials in liquid helium, provides generally acceptable predictions of initial crack size and ductile crack extension, and yields more conservative estimates of critical fracture toughness than the current ASTM E1820.

References

1. *Standard Test Method for Measurement of Fracture Toughness*, ASTM E1820-23b (West Conshohocken, PA: ASTM International, approved June 1, 2023), https://doi.org/10.1520/E1820-23B
2. B. Voss and R. A. Mayville, "The Use of the Partial Unloading Compliance Method for the Determination of JI-R Curves and JIc," in *Elastic-Plastic Fracture Test Methods: The User's Experience*, ed. F. J. Loss and E. T. Wessel (West Conshohocken, PA: ASTM International, 1985), 117–130, https://doi.org/10.1520/STP856-EB
3. B. Voss, "On the Problem of 'Negative Crack Growth' and 'Load Relaxation' in Single Specimen Partial Unloading Compliance Tests," in *Ductile Fracture Test Methods, Proceedings of a CSNI Workshop* (Paris: Nuclear Energy Agency, Organization for Economic Cooperation and Development, 1983), 54–60.
4. Y. A. Rosenthal, R. L. Tobler, and P. T. Purtscher, "J_{Ic} Data Analysis Methods with a 'Negative Crack Growth' Correction Procedure," *Journal of Testing and Evaluation* 18, no. 4 (July 1990): 301–304, http://doi.org/10.1520/JTE12488J
5. J. H. Underwood, E. J. Troiano, and R. T. Abbott, "Simpler J_{Ic} Test and Data Analysis Procedures for High-Strength Steels," in *Fracture Mechanics: Twenty-Fourth Volume*, ed. J. D. Landes, D. E. McCabe, and J. A. M. Boulet (West Conshohocken, PA: ASTM International, 1994), 410–421, https://doi.org/10.1520/STP1207-EB
6. C.-S. Seok, "Correction Methods of an Apparent Negative Crack Growth Phenomenon," *International Journal of Fracture* 102, no. 3 (April 2000): 259–269, https://doi.org/10.1023/A:1007680608587

7.   K. Weiss and A. Nyilas, "Specific Aspects on Crack Advance during *J*-Test Method for Structural Materials at Cryogenic Temperatures," *Fatigue & Fracture of Engineering Materials & Structures* 29, no. 2 (February 2006): 83–92, https://doi.org/10.1111/j.1460-2695.2006.00963.x

8.   M. A. Verstraete, S. Hertelé, R. M. Denys, K. Van Minnebruggen, and W. De Waele, "Evaluation and Interpretation of Ductile Crack Extension in SENT Specimens Using Unloading Compliance Technique," *Engineering Fracture Mechanics* 115 (January 2014): 190–203, https://doi.org/10.1016/j.engfracmech.2013.11.004

9.   P. Fernández-Pisón, J. A. Rodríguez-Martínez, E. García-Tabarés, I. Avilés-Santillana, and S. Sgobba, "Flow and Fracture of Austenitic Stainless Steels at Cryogenic Temperatures," *Engineering Fracture Mechanics* 258 (December 2021): 108042, https://doi.org/10.1016/j.engfracmech.2021.108042

10. J. D. Landes, Z. Zhou, K. Lee, and R. Herrera, "Normalization Method for Developing Curves with the Function," *Journal of Testing and Evaluation* 19, no. 4 (July 1991): 305–311, https://doi.org/10.1520/JTE12574J

11. *Method of Elastic-Plastic Fracture Toughness JIc Testing for Metallic Materials in Liquid Helium*, JIS Z 2284:1998 (E) (Tokyo, Japan: Japanese Standards Association, 1998).

12. G. Shen and W. R. Tyson, "Crack Length Evaluation for SE(T) Testing Using Unloading Compliance," *Journal of Testing and Evaluation* 37, no. 4 (July 2009): 347–357, https://doi.org/10.1520/JTE102368

13. ASTM International, "E08 Data Exchange," 2023, http://web.archive.org/web/20240110194821/https://www.astm.org/get-involved/technical-committees/adhoc-e08.html

14. E. Lucon, J. Benzing, and N. Hrabe, "Room Temperature Fracture Toughness Characterization of Additively Manufactured Ti-6Al-4V," *NIST Technical Note 2065* (Gaithersburg, MD: National Institute of Standards and Technology, 2019), https://doi.org/10.6028/NIST.TN.2065

15. H.-W. Viehrig, W. Baer, P. Gerwien, N. Grundmann, M. Houska, E. Lucon, T. Mottitschka, and P. Trubitz, "Bestimmung Der J-Risswiderstandskurve An Einem Zähen Reaktordruckbehälterstahl-Ergebnisse Eines Round Robin Tests," in *Proceedings of 45. Tagung des DVM-Arbeitskreises Bruchvorgänge, Bruchmechanische Werkstoff- und Bauteilbewertung: Beanspruchungsanalyse, Prüfmethoden und Anwendungen* (Berlin: Deutscher Verband für Materialforschung und-Prüfunge, 2013), 91–100.

16. J. Benzing, N. Derimow, E. Lucon, and T. Weeks, "*Fracture Toughness Tests at 77 K and 4 K on 316L Stainless Steel Welded Plates, NIST Technical Note 2230 (Superseded),*" (Gaithersburg, MD: National Institute of Standards and Technology, 2022), https://doi.org/10.6028/NIST.TN.2230

17. E. Lucon, T. S. Weeks, J. A. Gianetto, W. R. Tyson, and D. Y. Park, "Fracture Toughness Characterization of High-Pressure Pipe Girth Welds Using Single-Edge Notched Tension [SE(T)] Specimens," *Materials Performance and Characterization* 4, no. 2 (February 2015): 55–67, https://doi.org/10.1520/MPC20130098

Eqr{tki j v'd{'CUVO "Kpv\'cn'tki j w'tgugtxgf +'Ucv'Oct'2024'Material's'Performance and Characterization
Fqy pnqcf gf Ir tkpvgf 'd{'
WUC'F GRV'QH'EQO O GTEG/P KUV'r wtuwcpv'vq 'Nkegpug'Ci tggo gpv0P q 'hwt yj gt'tgr tqf wevkqpu'cwj qtk| gf 0